European Heart Journal (2013) **34**, 1122–1133
doi:10.1093/eurheartj/ehs226

Generation of patient-specific induced pluripotent stem cell-derived cardiomyocytes as a cellular model of arrhythmogenic right ventricular cardiomyopathy

Dongrui Ma[1], Heming Wei[1,2], Jun Lu[1], Shuswen Ho[1], Guangqing Zhang[1], Xiaoming Sun[1], Yingzi Oh[2], Suat Hoon Tan[3], Mah Lee Ng[3], Winston Shim[1], Philip Wong[1], and Reginald Liew[1,2]*

[1]Research and Development Unit (RDU), National Heart Centre Singapore, 17 Third Hospital Avenue, Singapore 168752, Singapore; [2]Duke-NUS Graduate Medical School, Singapore; [3]Electron Microscopy Unit and Department of Microbiology, Yong Loo Lin School of Medicine, National University of Singapore, Singapore

Received 23 April 2012; revised 21 June 2012; accepted 2 July 2012; online publish-ahead-of-print 13 July 2012

Aims Arrhythmogenic right ventricular cardiomyopathy (ARVC) is a primary heart muscle disorder associated with sudden cardiac death. Its pathophysiology is still poorly understood. We aimed to produce an *in vitro* cellular model of ARVC using patient-specific induced pluripotent stem cell (iPSC)-derived cardiomyocytes and determine whether the model could recapitulate key features of the disease phenotype.

Methods and results Dermal fibroblasts were obtained from a 30-year-old man with a clinical diagnosis of ARVC, harbouring a plakophilin 2 (PKP2) gene mutation. Four stable iPSC lines were generated using retroviral reprogramming, and functional cardiomyocytes were derived. Gene expression levels of desmosomal proteins (PKP2 and plakoglobin) in cardiomyocytes from ARVC–iPSCs were significantly lower compared with cardiomyocytes from control iPSCs ($P < 0.01$); there were no significant differences in the expression of desmoplakin, *N*-cadherin, and connexin 43 between the two groups. Cardiomyocytes derived from ARVC–iPSCs exhibited markedly reduced immunofluorescence signals when stained for PKP2 and plakoglobin, but similar levels of staining for desmoplakin, *N*-cadherin, and connexin 43 compared with control cardiomyocytes. Transmission electron microscopy showed that ARVC–iPSC cardiomyocytes were larger and contained darker lipid droplets compared with control cardiomyocytes. After 2 weeks of cell exposure to adiopgenic differentiation medium, ARVC–iPSC cardiomyocytes were found to contain a significantly greater amount of lipid, calculated using Oil Red O staining, compared with controls (734 ± 35.6 vs. 8.1 ± 0.49 a.u., respectively; $n = 7$, $P = 0.001$).

Conclusion Patient-specific iPSC-derived cardiomyocytes display key features of ARVC, including reduced cell surface localization of desmosomal proteins and a more adipogenic phenotype.

Keywords Induced pluripotent stem cells • Cardiomyocytes • Arrhythmogenic right ventricular cardiomyopathy

Introduction

Arrhythmogenic right ventricular cardiomyopathy (ARVC) is an inherited primary heart muscle disorder associated with a high risk of ventricular arrhythmias and sudden cardiac death. The classic histopathological hallmark is fibro-fatty infiltration of the myocardium, which can be detected on cardiac magnetic resonance imaging and from endomyocardial biopsy.[1] However, these findings may not be apparent in the early stages of the disease, during which patients may still be at risk of ventricular arrhythmias, leading to diagnostic difficulties and uncertainties. The genetic basis of ARVC is partially known, with ~40–50% of cases harbouring

* Corresponding author. Tel: +65 6436 7541, Fax: +65 6223 0972, Email: reginald.liew.k.c@nhcs.com.sg

mutations in genes coding for desmosomal proteins: desmoplakin, plakoglobin, plakophilin 2 (PKP2), desmoglein 2 (DSG2), and desmocollin 2 (DSC2).[2] Although animal models have provided some useful insights into the pathogenesis of ARVC, significant differences between the functional and electrophysiological properties of animal and human hearts impose limits on the interpretation and applicability of such data. In addition, the lack of good *in vitro* sources of living human cardiomyocytes and the failure to model patient-specific disease variations have markedly hindered the study of this disease.

In recent years, several groups have successfully modelled a number of inherited cardiac ion channel diseases, most notably different subtypes of long-QT syndrome, through the generation of patient-specific induced pluripotent stem cell (iPSC)-derived cardiomyocytes.[3–5] The objective of the present study was to investigate the feasibility of producing an *in vitro* cellular model of ARVC using patient-specific iPSC-derived cardiomyocytes, which could recapitulate key features of the disease phenotype. We hypothesized that iPSC-derived cardiomyocytes from ARVC patients would exhibit altered desmosomal protein localization at the intercalated discs and display a greater potential for adipocytic change compared with control cells. Successful generation of such a model would offer a unique platform to further our understanding of the pathogenesis of the disease as well as to evaluate future novel clinical applications in diagnosis and management.

Methods

Patient clinical details and genetic profile

The patient in this study was a 30-year-old Chinese man who had been diagnosed with ARVC based on international task force criteria (one major and two minor criteria). He was first referred for specialist cardiac assessment at the age of 25 in view of his strong family history of sudden cardiac death (his father and younger brother had died suddenly at the ages of 43 and 23, respectively). His ECG at presentation showed T-wave inversion in leads III, aVF, and V1 to V3 with normal QRS duration (*Figure 1*). Echocardiography showed a mildly dilated right ventricle with normal left ventricular size and function. Cardiac magnetic resonance scanning showed that the right ventricle was dilated and thinned with regional akinesia and reduced ejection fraction (41%); coronary angiography showed normal coronary arteries. Although he was initially asymptomatic at presentation, he developed episodes of palpitations and pre-syncope during the follow-up. Holter monitoring demonstrated frequent episodes of non-sustained ventricular tachycardia. Therefore, an implantable cardioverter defibrillator was inserted. Genetic testing revealed a heterozygous mutation in the PKP2 gene (c.1841T>C nucleotide change; *Figure 2A*); no other abnormalities were detected in the other genes tested that have been associated with ARVC (JUP, DSP, DSG2, DSC2, and TMEM43).

Generation of induced pluripotent stem cells

A 5 mm skin punch biopsy was taken from the patient with ARVC and a 32-year-old healthy male donor with no clinical history or manifestations of ARVC following informed consent. Skin dermis was manually separated, minced, and plated onto a Petri dish with Dulbecco's modified eagle medium (DMEM, Invitrogen, USA) (see Supplementary material online, Methods, for composition of all solutions used). Fibroblasts migrated out of the dermis tissue within 7 days and were subcultured weekly. Retrovirus containing pMXs-SOX2, pMXs-OCT3/4, pMXs-KLF4, and pMXs-C-MYC transgenes were packaged in HEK GP-293 cells (Clontech, USA) via calcium phosphate (Invitrogen)-mediated transfection. Colonies of iPSCs were picked after 3 weeks. Induced pluripotent stem cells were maintained in human embryonic stem cell (hESC) medium.

Induced pluripotent stem cell characterization and cardiac differentiation

The pluripotency of the iPSCs was confirmed using immunofluorescence staining and measuring gene expression of human pluripotent markers, performing DNA methylation assays and determining telomerase activity. Induced pluripotent stem cells were differentiated into cardiomyocytes through the formation of embryoid bodies (EBs) which were manually dissected after 21 days and dissociated. All cardiomyocytes used in subsequent experiments were 4–5 weeks following cardiac differentiation to ensure that they shared

Figure 1 Twelve-lead electrocardiography of patient with arrhythmogenic right ventricular cardiomyopathy.

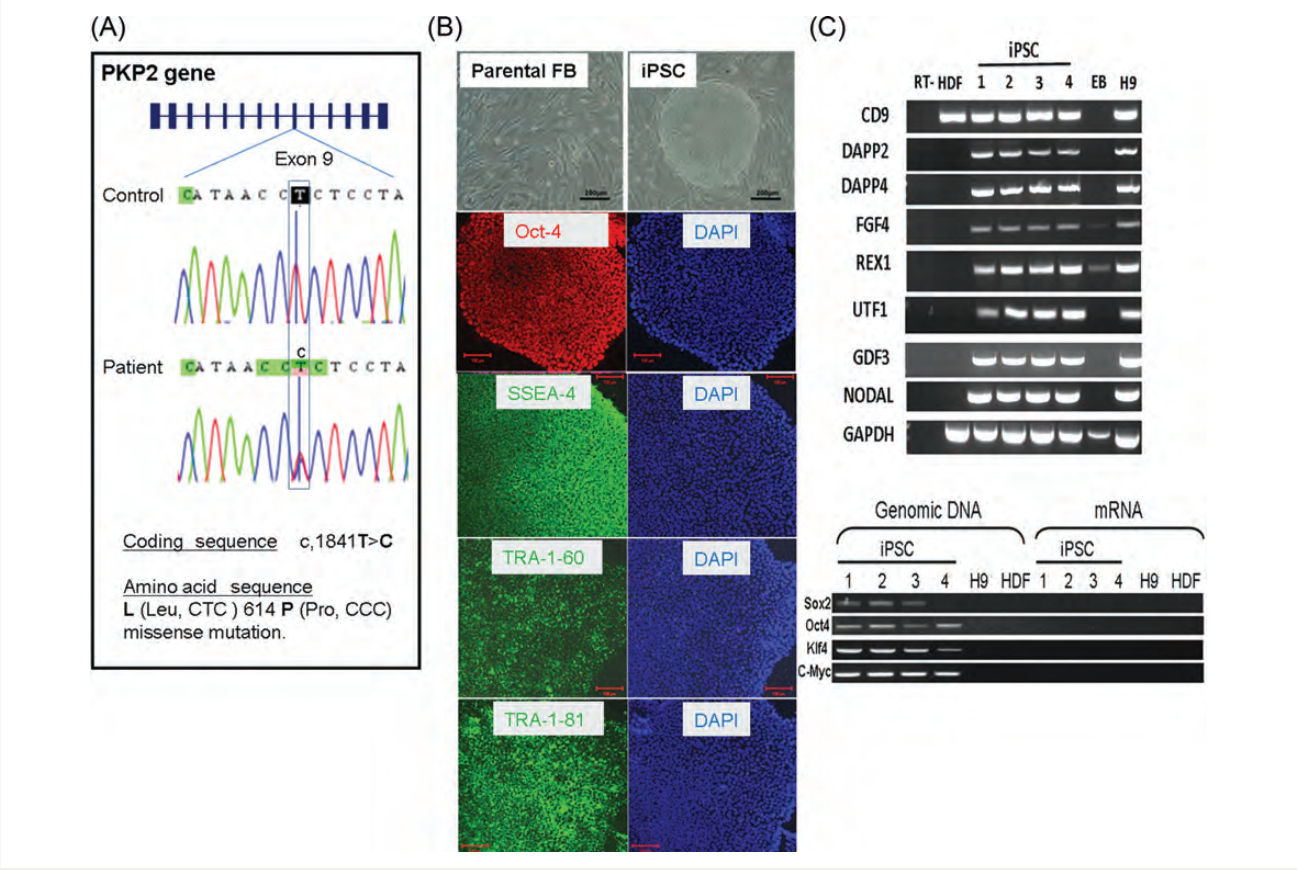

Figure 2 Genetic profile of the arrhythmogenic right ventricular cardiomyopathy (ARVC) patient and generation of induced pluripotent stem cells (iPSCs). (*A*) Schematic diagram showing the location of the plakophilin2 (PKP2) point mutation, resulting in an amino acid change from leucine to proline in position 614. (*B*) Morphology of patient dermal fibroblasts (upper left) and established arrhythmogenic right ventricular cardiomyopathy–induced pluripotent stem cell line at passage number 4, clone 1 (upper right). Immunofluorescence staining of Oct4, SSEA-4, TRA-1-60, and TRA-1-81 in arrhythmogenic right ventricular cardiomyopathy–induced pluripotent stem cells. Positive staining of Oct4 (red) was observed in cell nuclei, whereas positive staining of SSEA-4, TRA-1-60, and TRA-1-81 (green) were observed in the cell membrane. Cell nuclei were counter-stained with 4′,6-diamidino-2-phenylindole (DAPI, blue). Scale bars are 200 μm for upper photomicrographs and 100 μm for the immunofluorescence images. (*C*) Upper panel: polymerase chain reaction analysis of endogenous pluripotent genes in arrhythmogenic right ventricular cardiomyopathy–induced pluripotent stem cells. H9 human embryonic stem cells were used as a positive control and RT (−) was used as a negative control. Lower panel: polymerase chain reaction analysis for the expression of retroviral transgenes in arrhythmogenic right ventricular cardiomyopathy–induced pluripotent stem cells. Genomic DNA and mRNA were extracted from arrhythmogenic right ventricular cardiomyopathy–induced pluripotent stem cell clones 1 to 4, H9, and dermal fibroblasts (HDF). Retroviral transgenes of SOX2, OCT4, C-MYC, and KLF4 were only detected in genomic DNA of arrhythmogenic right ventricular cardiomyopathy–induced pluripotent stem cells.

similar maturity (see Supplementary material online, Methods, for more detail).

Characterization of induced pluripotent stem cell-derived cardiomyocytes

Single-cell patch-clamp recordings

Whole-cell patch-clamp recordings were performed on dissociated cardiomyocytes. Axopatch 200B, Digidata 1322, and pClamp10 (Molecular Devices, Sunnyvale, CA, USA) were used for data amplification, acquisition, and analysis. Action potential (AP) measurements were performed using the current clamp mode. The voltage-gated L-type calcium current (ICaL) was recorded in voltage-clamp mode using test pulses varying between −40 and +50 mV from a holding potential of −40 mV.

Laser confocal Ca^{2+} imaging for determining Ca^{2+} transients

Calcium imaging using confocal fluorescent microscopy was conducted on cardiomyocytes that were pre-loaded with 6 μg/mL Fluo-4 AM (Molecular Probes) for 15 min at 37°C and maintained in normal Tyrode solution. Ca^{2+} transients were recorded by an LSM-710 laser scanning confocal microscope (Carl Zeiss, Germany) with a ×40 oil immersion objective and a numeric aperture of 1.3. Fluo-4 was excited at 488 nm using a 25 mW argon laser (with intensity attenuated to 1%). Fluorescence emission was measured at >505 nm. Images were acquired in the line (X-T)-scan mode with 512 pixels per line at a rate of 3 ms per scan. The scan line was oriented along the longitudinal axis of the cell, at pixel intervals of 0.15 μm. The axial resolution was set at 1.5 μm according to the manufacturer's specifications. Ca^{2+} images were analysed using a computer program written in the IDL 5.4 software.

Cardiac and desmosomal gene expression profiling

The expression levels of desmosomal genes (plakoglobin, plakophilin2, *N*-cadherin, connexin43, and desmoplakin), α-actinin, β-myosin heavy chain (β-MHC), and GAPDH were determined in cardiomyocytes from ARVC–iPSCs and control–iPSCs using real-time polymerase chain reaction (PCR). The following measures were taken to improve the accuracy of the desmosomal gene profiling by eliminating the potential interfering of non-cardiomyocyte contamination: (i) total RNA was isolated from contracting cell clumps manually dissected from contracting EBs attached to cultural dish; (ii) expression levels of desmosomal genes were normalized to β-MHC and α-actinin levels. All primers and PCR conditions are shown in Supplementary material online, *Table S1*.

Immunofluorescence assays for cardiac contractile and desmosomal proteins

The identity and structural integrity of cardiomyocytes were determined by immunofluorescence staining for cardiac contractile proteins β-MHC and α-actinin. The intracellular localization of desmosomal proteins was determined by immunofluorescence with specific antibodies against desmosomal proteins. The mouse monoclonal antibodies used included anti-α-actinin (Sigma, USA), anti-β-MHC and connexin 43 (Millipore, USA), anti-plakoglobin (Sigma, USA), anti-plakophilin2, and *N*-cadherin; goat polyclonal antibody against desmoplakin (Santa Cruz, USA) was also used. All cardiomyocytes were counter-stained with antibodies against β-MHC and α-actinin to validate their cardiomyocyte identity and structural integration. The stained beating EBs and monolayer cell cultures were subjected to laser-scanning confocal microscopy (LSM710, Carl Zeiss) for recording pictures. The immunofluorescence results from iPSC-derived cardiomyocytes from the patient were compared with those of the control subject.

Transmission electron microscopy

Transmission electron microscopy (TEM) was performed on 4–5-week-old iPSC-derived cardiomyocytes from the patient and control subject (see Supplementary material online, Methods, for more detail). In each group of iPSC-derived cardiomyocytes, we chose cells to visualize the nucleus/nucleolae, myofilaments, and Z-bands. We also chose cells from control and patient-derived cardiomyocytes in which the desomosomal structures were clearly visible at the cell membranes. For semi-quantitative estimation of the number of lipid droplets present in control and ARVC–iPSC-derived cardiomyocytes, we counted the number of lipid droplets for six images (of the same magnification) and obtained an average number of lipid droplets per image.

Oil Red O staining and immunoperoxidase staining of α-actinin

To determine whether cells derived from the patient with ARVC had a greater adipogenic potential compared with control cells, we exposed patient and control cells to an environment that has been shown to induce stem cells into an adipocytic lineage.[6] Cardiomyocytes derived from ARVC– and control–iPSCs were seeded onto gelatin-coated dishes and incubated in adipogenic differentiation medium for 2 weeks as previously described.[6] The cell cultures were then fixed in 4% paraformaldehyde for 10 min at 4°C. Anti-α-actinin antibody (1:200, Sigma) was applied in 5% goat serum in PBS at room temperature for 45 min. Cells were washed with PBS three times and a biotinylated secondary antibody (Santa Cruz) applied for 30 min. The preparations were then incubated with avidin and biotinylated horseradish peroxidase and finally with peroxidase substrate for 5 min. To detect the lipid droplets within cells, Oil Red O staining was performed after immunoperoxidase staining. The cell cultures were rinsed with 60% isopropanol and stained with freshly prepared Oil Red O working solution for 15 min at room temperature. The cell cultures were then rinsed with distilled water, counter-stained with 4′,6-diamidino-2-phenylindole (DAPI; Burlingame, CA, USA) and mounted in aqueous mountant. Images were obtained using an Olympus CKX41 inverted fluorescent microscope.

Statistical analyses

Numerical data are presented as mean ± SEM. Comparisons between groups were evaluated with Student's *t*-test (two-tailed) using Microsoft Office Excel Professional 2010; $P < 0.05$ was considered significant.

Results

Patient-specific induced pluripotent stem cells and derived cardiomyocytes

We generated four iPSC lines from dermal fibroblasts obtained from the patient with ARVC, using retroviral reprogramming. Colonies with well-defined hESC morphology were selected and characterized (*Figure 2* and Supplementary material online, *Figures S1–S3*). Stable iPSC lines, clones 1 to 4, were obtained and maintained for more than 30 passages. The iPSC lines after four passages were used for subsequent studies. All these iPSCs uniformly expressed the pluripotency markers OCT4, SSEA-4, TRA-1-60, and TRA-1-81 as determined by immunofluorescence staining (*Figure 2B*). All the iPSC lines showed reactivation of the endogenous pluripotency-related genes CD9, DAPP2, DAPP4, FGF4, REX1, UTF1, GDF3, and NODAL, with similar levels of expression seen in hESCs (*Figure 2C*), analysed by RT-PCR. As expected, all the iPSC lines showed SOX-2, OCT-4, KLF-4, and C-MYC retroviral transgenes integration in genomic DNA with efficiently silenced expression as confirmed by RT-PCR (*Figure 2C*). In addition, all the iPSC lines showed demethylation of the OCT-4 promoter (Supplementary material online, *Figure S1*) and high levels of telomerase activity similar to that seen in hESCs (Supplementary material online, *Figure S2*). The pluripotency of the iPSCs produced was further confirmed upon injection of cells into the kidney capsule of immunocompromised SCID mice—all the iPSC lines generated teratomas, comprising structures and tissues derived from three embryonic germ layers, including glandular structure, cartilage, and neuroepithelium (Supplementary material online, *Figure S3*).

Electrophysiological characterization of single-arrhythmogenic right ventricular cardiomyopathy induced pluripotent stem cell-derived cardiomyocytes

The majority of ARVC patient iPSC-derived cardiomyocytes (>70%) exhibited a ventricular-like AP profile and the expected response following exposure to the calcium channel antagonist, nifedipine, and β-agonist, isoproterenol (*Figure 3A*). Thus, both the

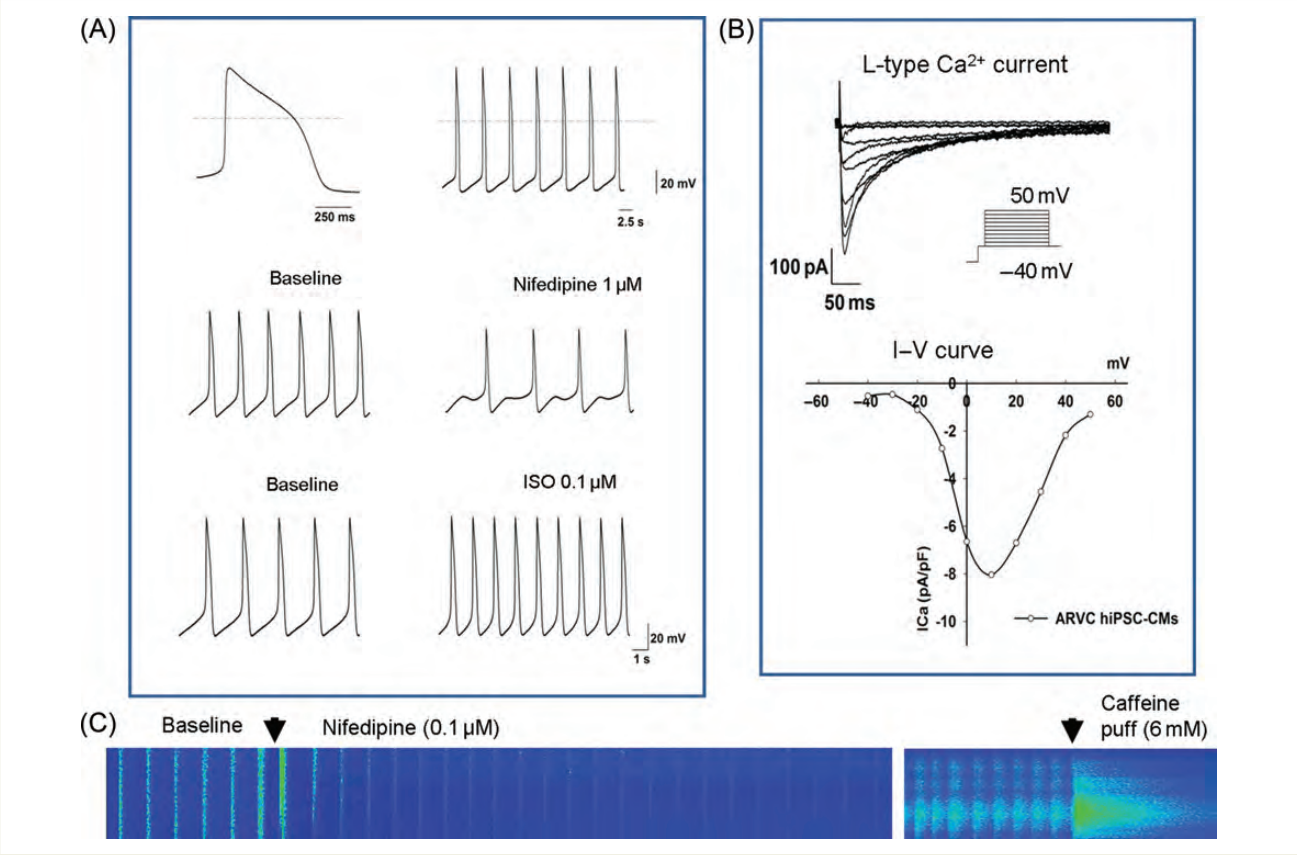

Figure 3 Electrophysiological characterization of induced pluripotent stem cell (iPSC)-derived cardiomyocytes from the arrhythmogenic right ventricular cardiomyopathy (ARVC)–induced pluripotent stem cells. (*A*) Action potential profile of a representative ventricular-like cell and its response to 1 μM nifedipine and 0.1 μM isoproterenol (ISO). (*B*) Representative L-type calcium current trace and *I–V* curve under voltage-clamp mode with a holding potential of −40 mV and test pulses from −40 to +50 mV. (*C*) Representative line-scan confocal calcium transients recorded with Flor-4-loaded cardiomyocytes at baseline and in the presence of 0.1 μM nifedipine (left). A line-scan image following a 6 μM caffeine puff is presented on the right.

rate of spontaneous cell contraction and contraction amplitude were reduced in the presence of 1 μM nifedipine, whereas contraction rate was increased in the presence of 0.1 μM isoproterenol. Cardiomyocytes exhibited a peak ICaL density of -8.0 ± 2.1 pA/pF (mean ± SEM, $n = 4$) from voltage-clamp studies (*Figure 3B*) and characteristic Ca^{2+} transients and responses to caffeine application (*Figure 3C*).

Quantification of desmosomal protein gene expression in cardiomyocytes

The transcript expression levels of PKP2 and plakoglobin in cardiomyocytes from ARVC–iPSCs were significantly lower compared with cardiomyocytes from control iPSCs ($P = 0.008$ and $P = 0.001$ for PKP2 and plakoglobin, respectively), although there were no significant differences in the expression of desmoplakin, *N*-cadherin, or connexin43 ($P > 0.05$) between ARVC and control groups (*Figure 4*). Gene expression was normalized to that of β-MHC and α-actinin (*Figure 4A* and *B*, respectively) to avoid interference from residual non-cardiomyocytes. No significant difference between the gene expression of β-MHC and α-actinin was observed between ARVC and control cardiomyocytes (data not shown).

Immunofluorescence staining for desmosomal proteins

The small clusters of contracting EBs in both groups showed positive staining for β-MHC and α-actinin, which is indicative of a cardiomyocyte identification (*Figure 5*). Cardiomyocytes derived from ARVC–iPSCs in EBs exhibited markedly reduced immunofluorescence signals when stained for PKP2 and plakoglobin, but similar levels of staining for desmoplakin, *N*-cadherin, and connexin 43 compared with control cardiomyocytes (*Figure 5*). To quantitatively compare desmosomal protein expression, monolayer cardiomyocytes were prepared from contracting cell clusters, and the staining intensity of desmosomal and structural proteins was quantified using the Image J software (http://rsbweb.nih.gov/ij/docs/examples/index.html). The results were compared between ARVC and control cardiomyocytes. The immunofluorescence staining performed in monolayer culture in both groups showed similar staining intensity for cardiac sarcomeric marker α-actinin.

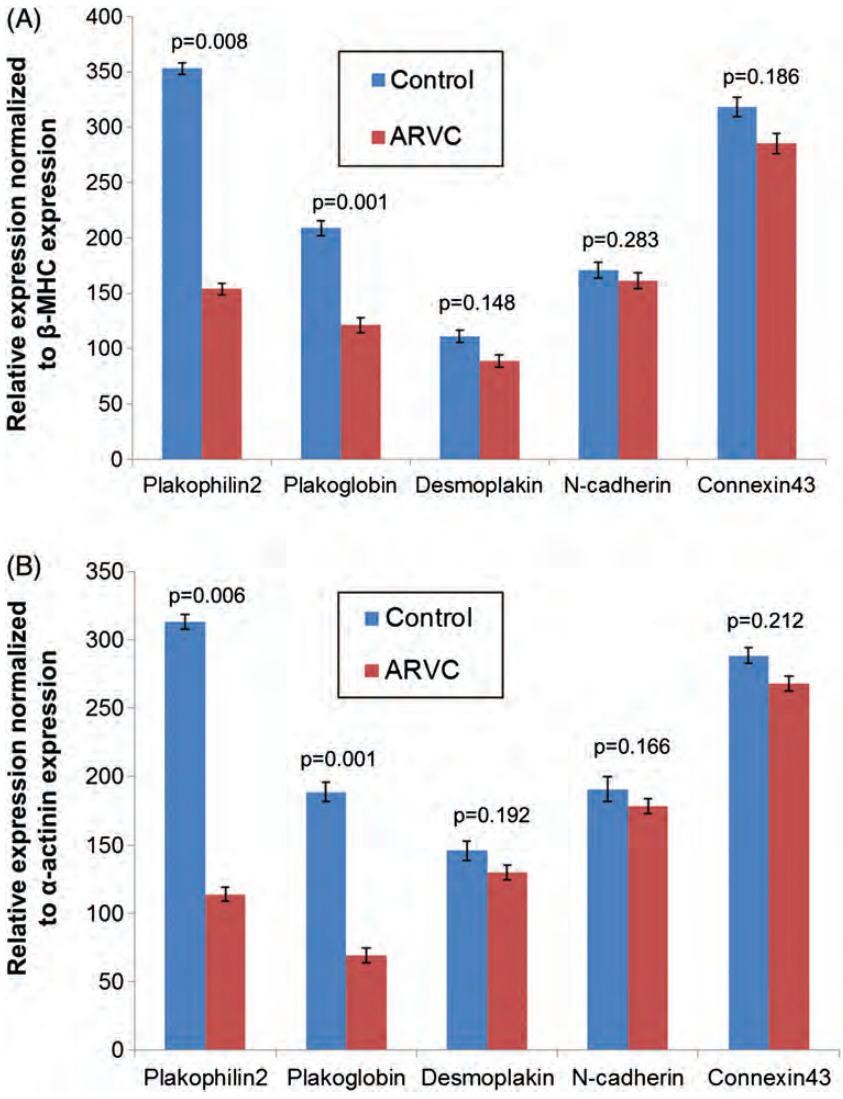

Figure 4 Detection of desmosomal gene expression in cardiomyocytes derived from arrhythmogenic right ventricular cardiomyopathy (ARVC)–induced pluripotent stem cells (iPSCs) and control–induced pluripotent stem cells. Real-time polymerase chain reaction was adopted to detect the gene expression of plakophilin2, plakoglobin, desmoplakin, *N*-cadherin, connexin43, β-myosin heavy chain (β-MHC), and α-actinin genes in cardiomyocytes derived from arrhythmogenic right ventricular cardiomyopathy and control–induced pluripotent stem cells. To exclude the interference of non-cardiomycytes, gene expression was normalized to that of β-myosin heavy chain and α-actinin. The gene expression of plakophilin2 and plakoglobin in cardiomyocytes from arrhythmogenic right ventricular cardiomyopathy–induced pluripotent stem cells was significantly lower than that of control–induced pluripotent stem cells ($P < 0.01$), although there were no significant differences in the expression of desmoplakin, *N*-cadherin, and connexin43 ($P > 0.05$) between arrhythmogenic right ventricular cardiomyopathy and control groups ($n = 5$ for each protein; triplicate for each experiment).

The immunofluorescence staining signals of PKP2 and plakoglobin were significantly reduced in the ARVC group, whereas the signals of the other proteins tested did not differ significantly between ARVC and control cells (*Figure 6*).

Ultrastructural analysis using transmission electron microscopy

Transmission electron microscopy of iPSC-derived cardiomyocytes from the control subject and patient with ARVC showed the ultrastructural integrity of the cells with myofibrils and Z-bands clearly visible (*Figure 7A*). The maximum cell width of ARVC–iPSC-derived cardiomyocytes was significantly greater than that of control cardiomyocytes (19.1 ± 1.0 vs. 12.3 ± 0.5 μm; $n = 7$, $P < 0.0001$). In addition, the Z-bands in ARVC–iPSC-derived cardiomyocytes appeared to be less organized, being thicker and more pleopmorphic compared with the Z-bands in control cells. In some images, desmosomes in ARVC–iPSC-derived cardiomyocytes appeared to be less dense in the cell peripheries compared with control cardiomyocytes (*Figure 7B*). There were no significant differences in the absolute

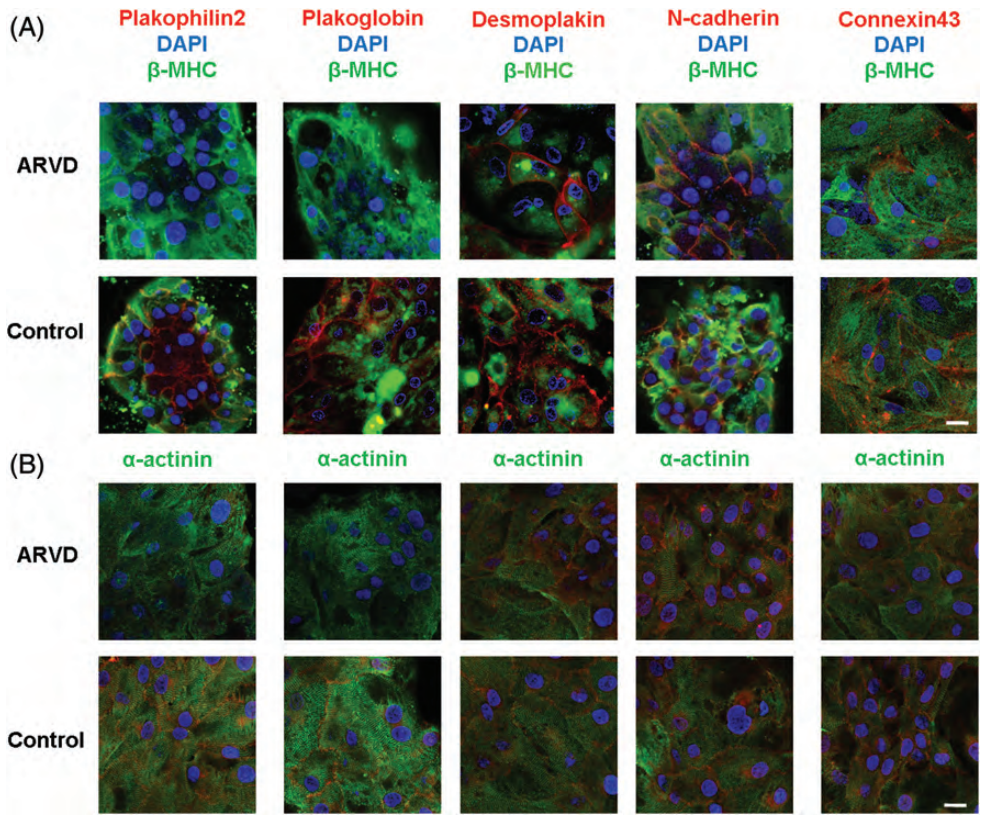

Figure 5 Immunofluorescence staining of desmosomal proteins in cardiomyocytes derived from arrhythmogenic right ventricular cardiomyopathy (ARVC)–induced pluripotent stem cells (iPSCs) and control–induced pluripotent stem cells. (*A*) Representative immunofluorescence images of induced pluripotent stem cell-derived cardiomyocytes in embryoid body from the arrhythmogenic right ventricular cardiomyopathy patient and control subject. The intercalated disc proteins of interest (plakophilin2, plakoglobin, desmoplakin, *N*-cadherin, and connexin 43) are stained red, β-myosin heavy chain (β-MHC) stained green, and cell nuclei stained blue with 4′,6-diamidino-2-phenylindole (DAPI). Scale bars = 50 μm. (*B*) Representative immunofluorescence images of induced pluripotent stem cell-derived cardiomyocytes in monolayer culture from the arrhythmogenic right ventricular cardiomyopathy patient and control subject. The intercalated disc proteins of interest are stained red, α-actinin stained green, and cell nuclei stained blue with 4′,6-diamidino-2-phenylindole. Scale bar = 20 μm.

number of lipid droplets per image between ARVC and control iPSC-derived cardiomyocytes on examination of six images in each group (27.7 ± 4.6 compared with 23.7 ± 1.8, mean ± SEM, respectively; $P = 0.43$). However, there seemed to be some visual differences in the morphology of the lipid droplets between the two groups, with lipid droplets appearing darker in patient-derived cardiomyocytes compared with control cells (*Figure 8B*).

Oil Red O staining

A significantly greater proportion of cardiomyocytes from ARVC–iPSCs stained positive (red colour) with Oil Red O compared with control cells (31.7 ± 1.48% vs. 10.34 ± 0.56%, respectively; $n = 7$, $P = 0.002$). Lipid droplets could be readily identified within the cells at high magnification (×20) (*Figure 9A*). For cardiomyocytes derived from ARVC– and control–iPSCs, the majority of cells were stained positive (dark brown/blue) for α-actinin, with striations clearly identified. Interestingly, for Oil Red O staining, dense positive staining (red) of lipid droplets could be seen in ARVC–iPSC-derived cardiomyocytes, whereas only sparse positive staining was observed within control-cardiomyocytes (*Figure 9B*). Quantitative calculation of Oil Red O staining intensity also showed a significantly greater intensity in ARVC–iPSC cardiomyocytes compared with controls (734 ± 35.6 vs. 8.1 ± 0.49 a.u., respectively; $n = 7$, $P = 0.001$).

Discussion

We have described for the first time the generation of iPSC-derived cardiomyocytes from a patient with a clinical diagnosis of ARVC and furthermore demonstrated significant phenotypic differences between cardiomyocytes from ARVC–iPSCs compared with control iPSCs. Cardiomyocytes from ARVC–iPSCs showed reduced gene expression of PKP2 and plakoglobin and reduced immunofluorescence signals for these desmosomal proteins at the cell periphery. Ultrastructural analyses of cardiomyocytes using TEM confirmed the structural integrity of the iPSC-derived cardiomocytes and provided some visual evidence for baseline differences in lipid droplets between ARVC– and control–iPSC-derived cardiomyocytes. Furthermore, we found that

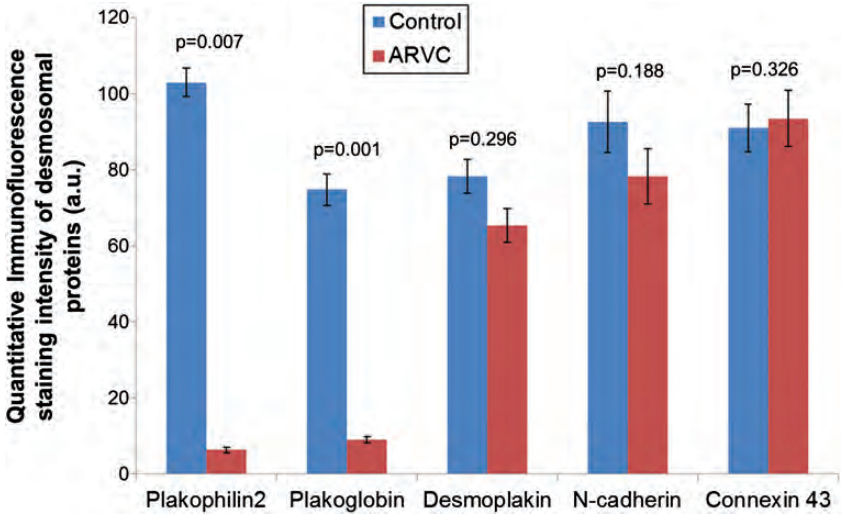

Figure 6 Quantitative calculation of immuofluorescence staining intensity of desmosomal proteins. The Image J software was used to quantitatively analyse the staining intensity of desmosomal proteins. The staining intensity was compared between cardiomyocytes from arrhythmogenic right ventricular cardiomyopathy (ARVC)–induced pluripotent stem cells and control–induced pluripotent stem cells. The immunofluorescence staining signals of plakophilin2 and plakoglobin were significantly reduced in the arrhythmogenic right ventricular cardiomyopathy group, whereas the signals of other proteins were not significantly different between arrhythmogenic right ventricular cardiomyopathy and control cells. a.u., arbitrary units.

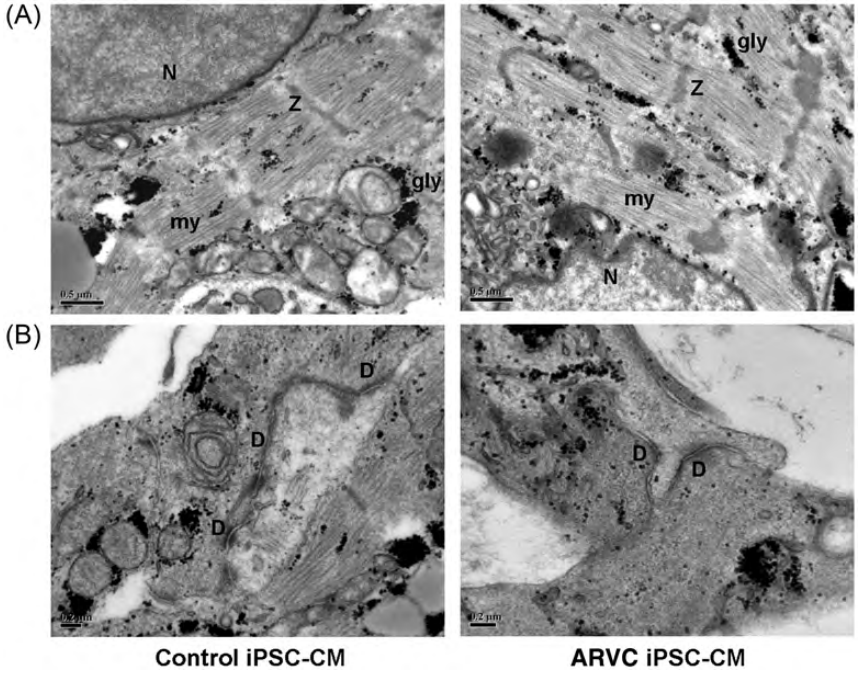

Figure 7 Transmission electron micrographs of cardiomyocytes derived from arrhythmogenic right ventricular cardiomyopathy (ARVC)–induced pluripotent stem cells (iPSCs) and control–induced pluripotent stem cells. (*A*) Representative images showing cardiomyocyte ultrastructure. Myofibrils (my) are organized in distinct sarcomeric structures delineated by Z-bands (Z). Glycogen masses (gly) are visible in the cytoplasm. N, nucleus. (*B*) Magnified view of cell membrane showing desmosomes (D) and junctional complexes.

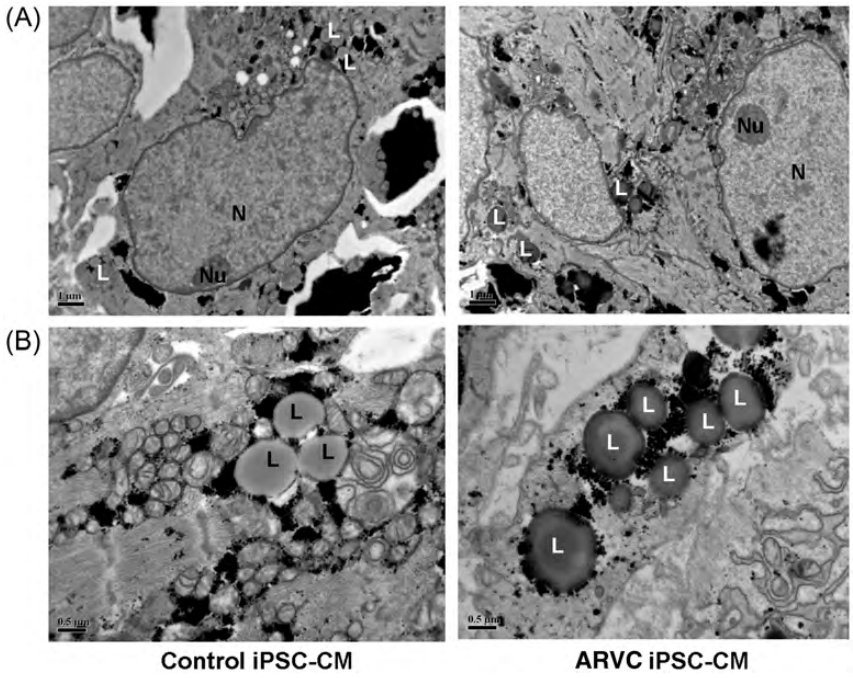

Figure 8 Transmission electron micrographs of induced pluripotent stem cell (iPSC)-derived cardiomyocytes showing lipid droplets in cell cytoplasm. (*A*) Small lipid droplets (L) seen relative to nucleus (N) and nucleolus (Nu) in induced pluripotent stem cell-derived cardiomyocytes from control subject (left) and patient with arrhythmogenic right ventricular cardiomyopathy (ARVC) (right). (*B*) Magnified view of cytoplasm showing lipid droplets in more detail. Induced pluripotent stem cell-derived cardiomyocytes from the arrhythmogenic right ventricular cardiomyopathy patient appeared to have darker lipid droplets compared with control cells.

cardiomyocytes from the patient with ARVC exhibited increased potential for adipocytic change when exposed to adipogenic differentiation medium for 2 weeks.

Correlation with clinical disease

Our findings of reduced desmosomal protein accumulation at the cell periphery are in close agreement with immunohistochemical results from human endomyocardial biopsy samples from ARVC patients[7] and open up the exciting possibility of using iPSC-derived cardiomyocytes from patients with ARVC as a cellular model to study the disease. We have also provided new data on the disease in two key respects: (i) gene expression of desmosomal proteins (specifically PKP2 and plakoglobin) was reduced in cardiomyocytes from ARVC–iPSCs, which is a possible explanation for the reduced immunofluorescence observed in the cells. In their study of human endomyocardial biopsy samples from ARVC patients, Asimaki *et al.*[7] did not specifically examine desmosomal gene expression and postulated that the reduction in plakoglobin signal levels at intercalated discs could be due to a redistribution of the protein from junctional to intracellular or intranuclear pools; (ii) we have provided evidence for increased adipogenic potential in cardiomyocytes from ARVC–iPSCs compared with control cells. This may underlie the predisposition to fibro-fatty change in the myocardium of patients with ARVC. However, the exposure of cells *in vitro* to an adipogenic differentiation medium is quite artificial and may not truly represent the situation in human disease in which fibro-fatty change of the myocardium often takes years to develop and may be influenced by a wide variety of endogenous and external factors. Clinical investigations performed on our patient did not show much evidence for fibro-fatty change and his predominant abnormality was electrical instability. It is questionable whether all the complexities and varying phenotypes of the disease, such as fibrofatty change and increased arrhythmogenicity, can be fully modelled by studying cardiomyocytes in isolation or from a single patient with a specific mutation and mode of presentation. It would be interesting to study other patients with ARVC with different mutations and clinical features, such as a predominantly fibro-fatty change in the myocardium, using this model. However, some clinical features of the disease, such as its predisposition to affecting the right ventricle and high pro-arrhythmic effects in some individuals (even before structural features become apparent), cannot be easily addressed using this model.

Comparison with other arrhythmogenic right ventricular cardiomyopathy models

Previous studies investigating the pathophysiology of ARVC have been hampered by the lack of good, genetically defined animal models. Arrhythmogenic right ventricular cardiomyopathy appears to occur spontaneously in Boxer dogs and is associated

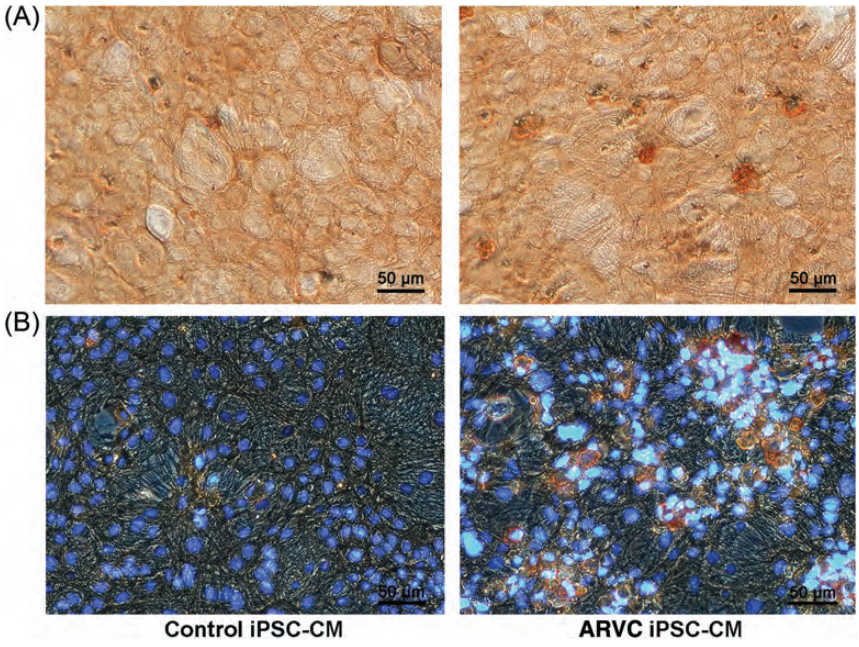

Figure 9 Oil Red O staining images cardiomyocytes from arrhythmogenic right ventricular cardiomyopathy (ARVC)– and control– induced pluripotent stem cells (iPSCs) after exposure to adipogenic differentiation medium for 2 weeks. (*A*) Images using Oil Red O staining only: a large proportion of cardiomyocytes from arrhythmogenic right ventricular cardiomyopathy–induced pluripotent stem cells stained positive for lipid droplets (dark red colour) within cells at high magnification (×20), whereas only a few control cells stained positive for lipids. Scale bar: 50 μm; ×20 magnification. (*B*) Cardiomyocytes (dark brown/blue) stained using anti-α-actinin, with striations clearly visible. In arrhythmogenic right ventricular cardiomyopathy–induced pluripotent stem cell-derived cardiomyocytes, Oil Red O staining revealed lipid droplets (red) within cells, whereas only sparse positive staining for lipid was observed within control-cardiomyocytes. Nuclei are stained light blue with 4′,6-diamidino-2-phenylindole (DAPI).

with ventricular arrhythmias and sudden cardiac death, although the genetic basis of the disease in these animals is unknown.[8] Murine models of ARVC involving specific mutations that result in some of the histopathological features seen in the human disease have been described and shed some light on disease mechanisms.[9,10] However, such models are limited by fundamental differences in cardiac electrophysiology between mice and humans and the general applicability of findings to human disease. Data from human endomyocardial biopsy samples taken from patients with ARVC have provided important insights into the structural changes that occur in the disease and relative distribution and complex binding interactions of proteins at the intercalated discs.[11] However, a limitation of this approach is that the cells and tissue are not usually viable. Hence, only structural, rather than functional, information can be obtained and mechanisms that require the study of living cells to unravel, such as alterations in cellular electrophysiology and cardiac ion channel function, cannot be elucidated. The appeal of a patient-specific iPSC-derived cellular model of ARVC, as we have described here, is that living human cells harbouring the genetic mutation(s) can be studied *in vitro* and used to provide both functional and structural data. In addition, patient-specific iPSCs, which harbour specific mutations, can be frozen and stored and potentially serve as an unlimited source of cells for future research and therapeutic applications.

PKP2 mutations and arrhythmogenic right ventricular cardiomyopathy

The patient used in this study harboured a heterozygous PKP2 mutation (c.1841T>C nucleotide change) which has not previously been described. Other investigators have reported PKP2 mutations in patients and families of western descent with ARVC, in which the mutations demonstrate variable penetrance and phenotypic expression of the disease.[12–14] In a study of 56 index cases of ARVC in a Dutch cohort fulfilling the published task force criteria, van Tintelen *et al.*[14] identified 14 different (11 novel) PKP2 mutations in 24 subjects (43%). Similarly, Gerull *et al.*[15] identified heterozygous mutations in PKP2 in 32 of 120 unrelated individuals with ARVC and found incomplete penetrance in most carriers in two kindreds. It is likely that our patient, being of Chinese ethnicity and with a definite clinical diagnosis of ARVC according to task force criteria, has a novel heterozygous PKP2 mutation which may be related to the pathogenesis of ARVC (mutation analysis for all the other genes known to be associated with ARVC were negative). The clinical features of T-wave inversion in the right precordial leads and right ventricular abnormality on cardiac imaging in our patient are similar to the clinical features described in ARVC patients from Greece and Cyprus who also have PKP2 mutations.[16] However, it is not established whether the particular PKP2 mutation observed in our patient is *causally* related to ARVC (our

patient has no other living first-degree relatives for which we could obtain DNA). The mutation has therefore been classified as unclassified variant type 3 (UV3), i.e. likely pathogenic but not confirmed.

It is interesting that in our model, plakoglobin gene expression and immunofluorescence levels for plakoglobin were also reduced, even though our patient did not have any of the known plakoglobin mutations when tested for them. PKP2 and plakoglobin are armadillo proteins located at the outer dense plaque of desmosomes, which are intricately co-related and share mutual molecular interations.[17,18] It is possible that reduced PKP2 levels can also result in reduced co-localization of plakoglobin, even though the patient may not have a mutation of the plakoglobin gene. In addition, loss of plakoglobin at the intercalated disc may be a final common pathway for ARVC and has been observed in patients with desmosomal mutations other than plakoglobin mutations.[19,20]

Study limitations

A number of limitations exist with our *in vitro* cellular model, which should be recognized. First, it is likely that important cell–cell interactions also exist and that cells other than cardiomyocytes may be relevant to the pathogenesis of ARVC; both of these factors cannot be modelled simply using a cellular platform. Our model could potentially be modified to study cell–cell interactions by incorporating the cardiomyocytes into cardiac cell sheets, which have been shown to beat spontaneously and synchronously with murine embryonic stem cell-derived cardiomyocytes.[21] Another limitation includes the difficulty of modelling a predominantly adult-onset disease using iPSC-derived cardiomyocytes, which still possess some foetal-like characteristics. Further *in vitro* manipulation of iPSC-derived cardiomyocytes to generate cells with a more mature phenotype may be required in order to successfully model other aspects of the disease. This may involve measures such as manipulation of the Wnt/β-catenin signalling pathway.[22,23]

Conclusions

We have demonstrated that iPSC-derived cardiomyocytes generated from a patient with ARVC display some of the key features of the disease, namely reduced cell surface localization of desmosomal proteins and a more adipogenic phenotype. These patient-specific cells may therefore be a useful addition to the current tools available to study this complex disease. Further mechanistic studies using iPSC-derived cardiomyocytes generated from other patients with ARVC, including those harbouring other desmosomal protein mutations, are required to determine the true potential of this approach in shedding additional insights into this disease.

Supplementary material

Supplementary material is available at *European Heart Journal* online.

Funding

The work in this study was funded by the Goh Foundation Cardiovascular Research award.

Conflict of interest: none declared.

References

1. Sen-Chowdhry S, Morgan RD, Chambers JC, McKenna WJ. Arrhythmogenic cardiomyopathy: etiology, diagnosis, and treatment. *Annu Rev Med* 2010;**61**:233–253.
2. Lombardi R, Marian AJ. Arrhythmogenic right ventricular cardiomyopathy is a disease of cardiac stem cells. *Curr Opin Cardiol* 2010;**25**:222–228.
3. Moretti A, Bellin M, Welling A, Jung CB, Lam JT, Bott-Flugel L, Dorn T, Goedel A, Höhnke C, Hofmann F, Seyfarth M, Sinnecker D, Schömig A, Laugwitz KL. Patient-specific induced pluripotent stem-cell models for long-QT syndrome. *N Engl J Med* 2010;**363**:1397–1409.
4. Itzhaki I, Maizels L, Huber I, Zwi-Dantsis L, Caspi O, Winterstern A, Feldman O, Gepstein A, Arbel G, Hammerman H, Boulos M, Gepstein L. Modelling the long QT syndrome with induced pluripotent stem cells. *Nature* 2011;**471**:225–229.
5. Oh Y, Wei H, Ma D, Sun X, Liew R. Clinical applications of patient-specific induced pluripotent stem cells in cardiovascular medicine. *Heart* 2012;**98**:443–449.
6. Pittenger MF, Mackay AM, Beck SC, Jaiswal RK, Douglas R, Mosca JD, Moorman MA, Simonetti DW, Craig S, Marshak DR. Multilineage potential of adult human mesenchymal stem cells. *Science* 1999;**284**:143–147.
7. Asimaki A, Tandri H, Huang H, Halushka MK, Gautam S, Basso C, Thiene G, Tsatsopoulou A, Protonotarios N, McKenna WJ, Calkins H, Saffitz JE. A new diagnostic test for arrhythmogenic right ventricular cardiomyopathy. *N Engl J Med* 2009;**360**:1075–1084.
8. Basso C, Fox PR, Meurs KM, Towbin JA, Spier AW, Calabrese F, Maron BJ, Thiene G. Arrhythmogenic right ventricular cardiomyopathy causing sudden cardiac death in Boxer dogs: a new animal model of human disease. *Circulation* 2004;**109**:1180–1185.
9. Asano Y, Takashima S, Asakura M, Shintani Y, Liao Y, Minamino T, Asanuma H, Sanada S, Kim J, Ogai A, Fukushima T, Oikawa Y, Okazaki Y, Kaneda Y, Sato M, Miyazaki J, Kitamura S, Tomoike H, Kitakaze M, Hori M. Lamr1 functional retroposon causes right ventricular dysplasia in mice. *Nat Genet* 2004;**36**:123–130.
10. Yang Z, Bowles NE, Scherer SE, Taylor MD, Kearney DL, Ge S, Nadvoretskiy VV, DeFreitas G, Carabello B, Brandon LI, Godsel LM, Green KJ, Saffitz JE, Li H, Danieli GA, Calkins H, Marcus F, Towbin JA. Desmosomal dysfunction due to mutations in desmoplakin causes arrhythmogenic right ventricular dysplasia/cardiomyopathy. *Circ Res* 2006;**99**:646–655.
11. Saffitz JE, Asimaki A, Huang H. Arrhythmogenic right ventricular cardiomyopathy: new insights into mechanisms of disease. *Cardiovasc Pathol* 2010;**19**:166–170.
12. Aneq MA, Fluur C, Rehnberg M, Soderkvist P, Engvall J, Nylander E, Gunnarsson C. Novel plakophilin2 mutation: three-generation family with arrhythmogenic right ventricular cardiomyopathy. *Scand Cardiovasc J* 2011;**46**:72–75.
13. Kannankeril PJ, Bhuiyan ZA, Darbar D, Mannens MM, Wilde AA, Roden DM. Arrhythmogenic right ventricular cardiomyopathy due to a novel plakophilin 2 mutation: wide spectrum of disease in mutation carriers within a family. *Heart Rhythm* 2006;**3**:939–944.
14. van Tintelen JP, Entius MM, Bhuiyan ZA, Jongbloed R, Wiesfeld AC, Wilde AA, van der Smagt J, Boven LG, Mannens MM, van Langen IM, Hofstra RM, Otterspoor LC, Doevendans PA, Rodriguez LM, van Gelder IC, Hauer RN. Plakophilin-2 mutations are the major determinant of familial arrhythmogenic right ventricular dysplasia/cardiomyopathy. *Circulation* 2006;**113**:1650–1658.
15. Gerull B, Heuser A, Wichter T, Paul M, Basson CT, McDermott DA, Lerman BB, Markowitz SM, Ellinor PT, MacRae CA, Peters S, Grossmann KS, Drenckhahn J, Michely B, Sasse-Klaassen S, Birchmeier W, Dietz R, Breithardt G, Schulze-Bahr E, Thierfelder L. Mutations in the desmosomal protein plakophilin-2 are common in arrhythmogenic right ventricular cardiomyopathy. *Nat Genet* 2004;**36**:1162–1164.
16. Antoniades L, Tsatsopoulou A, Anastasakis A, Syrris P, Asimaki A, Panagiotakos D, Zambartas C, Stefanadis C, McKenna WJ, Protonotarios N. Arrhythmogenic right ventricular cardiomyopathy caused by deletions in plakophilin-2 and plakoglobin (Naxos disease) in families from Greece and Cyprus: genotype–phenotype relations, diagnostic features and prognosis. *Eur Heart J* 2006;**27**:2208–2216.
17. Zhurinsky J, Shtutman M, Ben-Ze'ev A. Plakoglobin and beta-catenin: protein interactions, regulation and biological roles. *J Cell Sci* 2000;**113**:3127–3139.
18. Al-Amoudi A, Castano-Diez D, Devos DP, Russell RB, Johnson GT, Frangakis AS. The three-dimensional molecular structure of the desmosomal plaque. *Proc Natl Acad Sci USA* 2011;**108**:6480–6485.
19. Gehmlich K, Syrris P, Peskett E, Evans A, Ehler E, Asimaki A, Anastasakis A, Tsatsopoulou A, Vouliotis AI, Stefanadis C, Saffitz JE, Protonotarios N, McKenna WJ. Mechanistic insights into arrhythmogenic right ventricular cardiomyopathy caused by desmocollin-2 mutations. *Cardiovasc Res* 2011;**90**:77–87.

20. Asimaki A, Saffitz JE. The role of endomyocardial biopsy in ARVC: looking beyond histology in search of new diagnostic markers. *J Cardiovasc Electrophysiol* 2011;**22**:111–117.
21. Matsuura K, Masuda S, Haraguchi Y, Yasuda N, Shimizu T, Hagiwara N, Zandstra PW, Okano T. Creation of mouse embryonic stem cell-derived cardiac cell sheets. *Biomaterials* 2011;**32**:7355–7362.
22. Paige SL, Osugi T, Afanasiev OK, Pabon L, Reinecke H, Murry CE. Endogenous Wnt/beta-catenin signaling is required for cardiac differentiation in human embryonic stem cells. *PLoS One* 2010;**5**:e11134.
23. Lombardi R, da Graca Cabreira-Hansen M, Bell A, Fromm RR, Willerson JT, Marian AJ. Nuclear plakoglobin is essential for differentiation of cardiac progenitor cells to adipocytes in arrhythmogenic right ventricular cardiomyopathy. *Circ Res* 2011;**109**:1342–1353.

CARDIOVASCULAR FLASHLIGHT

doi:10.1093/eurheartj/ehs479
Online publish-ahead-of-print 9 January 2013

Arterial elongation and tortuosity leads to detection of a *de novo TGFBR2* mutation in a young patient with complex aortic pathology

Koen M. van de Luijtgaarden[1], Frederico Bastos Gonçalves[1,2], Danielle Majoor-Krakauer[3], and Hence J.M. Verhagen[1]*

[1]Department of Vascular Surgery, Erasmus University Medical Center, Suite H-810, PO Box 2040, 3000 CA Rotterdam, The Netherlands; [2]Department of Angiology and Vascular Surgery, Hospital de Santa Marta, CHLC, Lisbon, Portugal; and [3]Department of Clinical Genetics, Erasmus University Medical Center, Rotterdam, The Netherlands

* Corresponding author. Tel: +31 10 703 1810, Fax: +31 10 703 2396, Email: h.verhagen@erasmusmc.nl

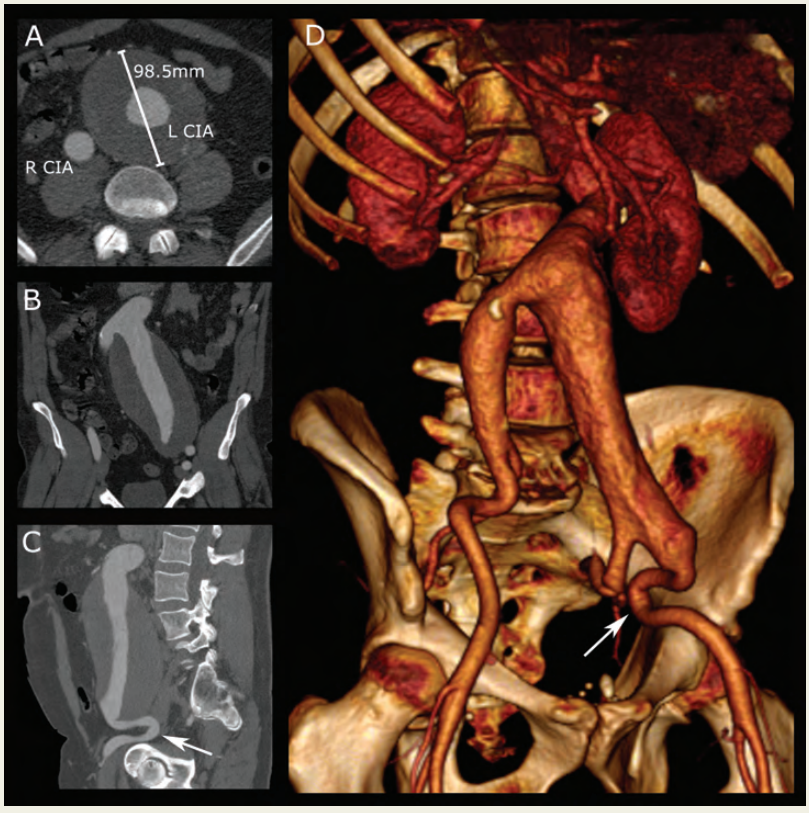

In a 47-year-old muscular-build male admitted with acute abdominal pain imaging revealed a Stanford type-B aortic dissection associated with a pre-existing large aorto-iliac aneurysm (*Panels A* and *B*) and marked iliac-artery elongation and tortuosity (*Panels C* and *D*, arrows). The patient underwent uneventful elective open repair of the aorto-iliac aneurysm. The marked aortic elongation and tortuosity at a young age in this patient prompted referral for genetic counselling after surgery. No characteristic facial or musculoskeletal signs of Loeys-Dietz or Marfan syndrome were present and there was no family history of vascular disease. Nevertheless, DNA analysis showed a '*de-novo*' *TGFBR2* mutation.

Arterial elongation and tortuosity is a main feature in patients with characteristic facial and musculoskeletal appearance of the TGF-β pathway-related genetic aneurysm syndromes. Therefore, our observation expands the phenotypic spectrum of TGF-β pathway-related pathology to patients with severe abdominal and iliacal arterial disease without major dysmorphological characteristics.

We demonstrate the importance of genetic testing in younger patients presenting with complex aortic pathology with marked arterial elongation and tortuosity, even in the absence of characteristic phenotypic features of a genetic aneurysm syndrome or a family history of aortic aneurysms. Correct genetic diagnosis of *TGFBR2*-related aortic pathology is important for clinical management of the patients and for genetic counselling of the family. Since *TGFBR2*-linked genetic aneurysms have an autosomal dominant inheritance, relatives at risk should be offered genetic counselling and pre-symptomatic testing for *TGFBR2* mutations. In this way, carriers of the *TGFBR2* mutation can benefit from screening and timely intervention.

This work was supported by an unrestricted grant from the 'Lijf & Leven' Foundation, Rotterdam, The Netherlands.